

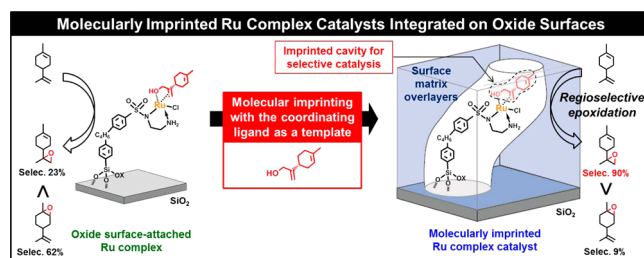
Molecularly Imprinted Ru Complex Catalysts Integrated on Oxide Surfaces

SATOSHI MURATSUGU AND MIZUKI TADA*

*Institute for Molecular Science and Department of Structural Molecular Science,
The Graduate University for Advanced Studies (SOKENDAI), 38 Nishigo-naka,
Myodaiji, Okazaki, Aichi 444-8585, Japan*

RECEIVED ON MAY 11, 2012

CONSPECTUS



Selective catalysis is critical for the development of green chemical processes, and natural enzymes that possess specialized three-dimensional reaction pockets with catalytically active sites represent the most sophisticated systems for selective catalysis. A reaction space in an enzyme consists of an active metal center, functional groups for molecular recognition (such as amino acids), and a surrounding protein matrix to prepare the reaction pocket. The artificial design of such an integrated catalytic unit in a non-enzymatic system remains challenging. Molecular imprinting of a supported metal complex provides a promising approach for shape-selective catalysis. In this process, an imprinted cavity with a shape matched to a template molecule is created in a polymer matrix with a catalytically active metal site.

In this Account, we review our studies on molecularly imprinted metal complex catalysts, focusing on Ru complexes, on oxide surfaces for shape-selective catalysis. Oxide surface-attached transition metal complex catalysts not only improve thermal stability and catalyst dispersion but also provide unique catalytic performance not observed in homogeneous precursors. We designed molecularly imprinted Ru complexes by using surface-attached Ru complexes with template ligands and inorganic/organic surface matrix overlayers to control the chemical environment around the active metal complex catalysts on oxide surfaces. We prepared the designed, molecularly imprinted Ru complexes on SiO₂ surfaces in a step-by-step manner and characterized them with solid-state (SS) NMR, diffuse-reflectance (DR) UV-vis, X-ray photoelectron spectroscopy (XPS), Brunauer–Emmett–Teller isotherm (BET), X-ray fluorescence (XRF), and Ru K-edge extended X-ray absorption fine structure (EXAFS). The catalytic performances of these Ru complexes suggest that this process of molecular imprinting facilitates the artificial integration of catalytic functions at surfaces. Further advances such as the imprinting of a transition state structure or the addition of multiple binding sites could lead to systems that can achieve 100% selective catalysis.

1. Introduction

The pursuit of selective artificial catalysts is a long-standing challenge. Natural enzymes are sophisticated catalytic systems capable of molecular recognition, and they are role models of catalysts that are selective for particular reactants. Enzymes use specialized three-dimensional active sites to control and carry out catalytic reactions. The design of such active sites in nonenzymatic systems remains a challenging endeavor.

Molecular imprinting^{1,2} is a method for creating, in a polymer matrix, an imprinted cavity that has a shape matched to a template molecule. Molecular imprinting has been initially developed for polymer science and analytical applications^{3–10} and has also been applied to the preparation of shape-selective catalysts by incorporating catalytically active sites.^{11–19} An organic or inorganic monomer is polymerized in the presence of a template, and subsequent removal of the template from the prepared

polymer matrix produces a molecularly imprinted cavity with a shape matched to the template molecule. Molecular imprinting of a metal complex whose ligand is utilized as the template is practical for controlling the chemical environment around the metal complex catalysts in an imprinted cavity and for enhancing catalytic properties (activity, selectivity, and stability).^{12–18}

Most imprinted metal complex catalysts are prepared by imprinting in bulk organic polymers,^{12,14–18} which often hinders access of reactant molecules to reaction sites contained within. A supported metal complex has an advantage over the corresponding homogeneous catalysts in that the site isolation effect provides stability to the metal complex, and unique catalytic performance is realized through the interplay between the attached metal complex and the support surface.^{20–25} We have developed an approach that combines a supported metal complex and molecular imprinting to produce shape-selective reaction sites for particular molecules by using ligands on the metal center as a template for selective catalysis as summarized in Scheme 1. Molecularly imprinted Rh dimer and monomer catalysts on SiO₂ exhibited remarkable performances for shape-selective hydrogenation of alkenes.^{26–29}

This Account highlights our recent work on molecularly imprinted Ru complex catalysts on oxide surfaces.^{30,31} The following six factors are essential in achieving integrated catalysis on such catalysts: (1) conformation of ligands on the metal complex, (2) orientation of the vacant site (cavity) with respect to the metal center, (3) shape of the imprinted cavity, (4) wall of the matrix overlayers to regulate the mobility of the supported metal complex, (5) surface micropores for access of reactants to the active metal complex, and (6) molecular binding site on the matrix overlayers. Toward the preparation of artificial enzymatic surfaces for selective catalysis, the design of molecularly imprinted metal complex catalysts on oxide surfaces enables the integration of catalytic functions at the surfaces.

2. Molecularly Imprinted Ru Complexes with SiO₂-Matrix Overlayers for Regioselective Epoxidation

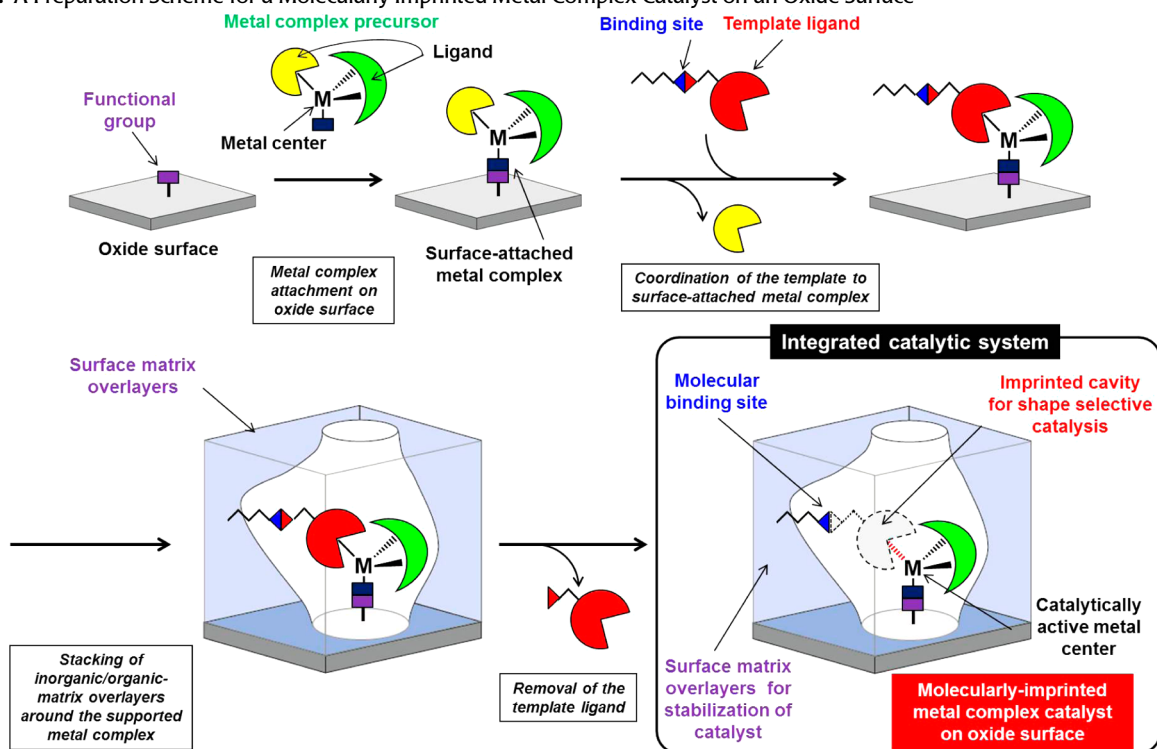
Regioselective intramolecular reactions are an important target in that they accomplish a pinpoint functional group transformation at a particular position without the need for protecting groups elsewhere in the molecule. We have applied our approach of designing a molecularly imprinted metal complex catalyst whose ligand is similar in shape to the reaction intermediate or product of a particular functional group transformation in a regioselective intramolecular reaction.

A target reaction was the regioselective epoxidation of (*R*)-(+)-limonene: a molecule with one internal C=C bond and one terminal C=C bond. Both C=C bonds react with an appropriate oxidant to produce the internal epoxide, the terminal epoxide, or the diepoxide. In general, the epoxidation of an internal alkene is faster than that of a terminal alkene, resulting in low selectivity for the terminal epoxide. We applied the molecular imprinting technique to a SiO₂-supported Ru complex, which is active for the epoxidation of alkenes,^{32–34} and prepared molecularly imprinted Ru complex catalysts for the regioselective epoxidation of the terminal C=C bond of (*R*)-(+)-limonene by using limonen-10-ol, which serves as an isostructural template for the epoxidation of the terminal alkene of (*R*)-(+)-limonene.

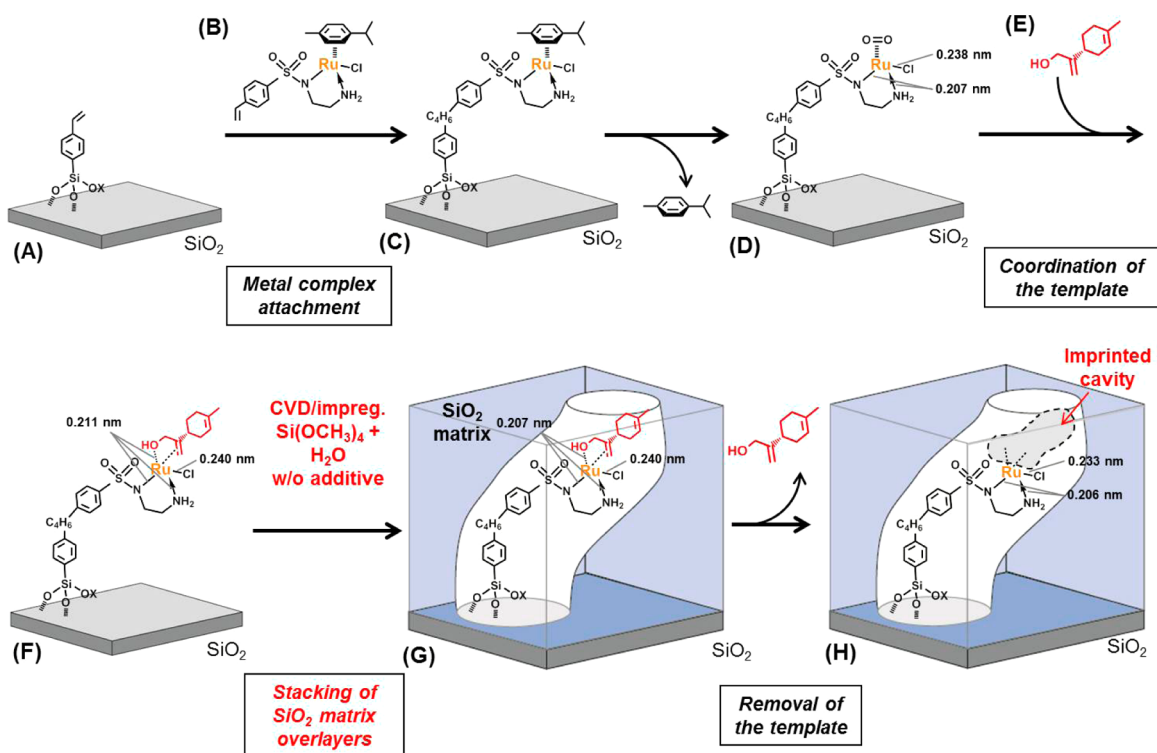
Scheme 2 shows the steps for preparing the molecularly imprinted Ru complex designed for the regioselective epoxidation of the terminal alkene of (*R*)-(+)-limonene. A site-isolated Ru complex was prepared on a SiO₂ surface; a Ru complex precursor (**B**) was grafted onto *p*-styryl-functionalized SiO₂ (**A**), and the supported Ru complex (**D**) was prepared.^{32–34} Then, the template limonen-10-ol (**E**) (0.8 equiv with respect to Ru) was coordinated to **D**, as characterized by ¹³C solid-state (SS) NMR (Figure 1) and Ru K-edge extended X-ray absorption fine structure (EXAFS) (Table S1, Supporting Information). In the ¹³C SS-NMR spectrum, six peaks attributable to **E** were clearly observed for the SiO₂-supported Ru complex with the template (**F**): 28.2, 36.9, 65.2, 107.8, 120.4, and 133.8 ppm (Figure 1).

Surface SiO₂-matrix overlayers were stacked on the SiO₂ surface with the Ru complex, and space around the supported Ru complex was covered by the matrix overlayers. The SiO₂-matrix overlayers can be prepared by chemical vapor deposition (CVD) of Si(OCH₃)₄ (TMOS) and H₂O and subsequent hydrolysis polymerization, and a SiO₂ network with many hydroxyl groups, which were observed by ²⁹Si SS-NMR (Figure 2), was formed.^{26–29} The SiO₂-matrix overlayers had a micropore structure, the diameter of which was estimated to be 0.73 nm by Brunauer–Emmett–Teller isotherm (BET) analysis. We found that the addition of basic organosilane coupling agents led to the formation of a more rigid SiO₂ network with better regioselectivity for epoxidation of the terminal C=C bond of (*R*)-(+)-limonene. A small amount of organosilane coupling agent or organic reagent triethoxy-3-(2-imidazolyl)propylsilane (IM-Si), (*N,N*-dimethylaminopropyl)trimethoxysilane (NMe₂-Si), (3-aminopropyl)trimethoxysilane (NH₂-Si), *p*-styryltrimethoxysilane (*p*-styryl-Si), 1-methyl-3-[3-(triethoxysilyl)propyl]imidazolium chloride (IL-Si), 4-[*N*-[3-(triethoxysilyl)propyl]-*N*-methylamino]-

SCHEME 1. A Preparation Scheme for a Molecularly Imprinted Metal Complex Catalyst on an Oxide Surface



SCHEME 2. Steps for Preparing the Molecularly Imprinted Ru Complex Catalyst for Selective Epoxidation of the Terminal C=C Bond of (R)-(+)-Limonene



pyridine (DMAP-Si), ammonia (NH_3), trimethylamine (NMe_3), 2-methylimidazole (2-MeIM), 4-(*N*-methylamino)pyridine

(MAP); <2 wt %) was impregnated together with TMOS and H_2O .

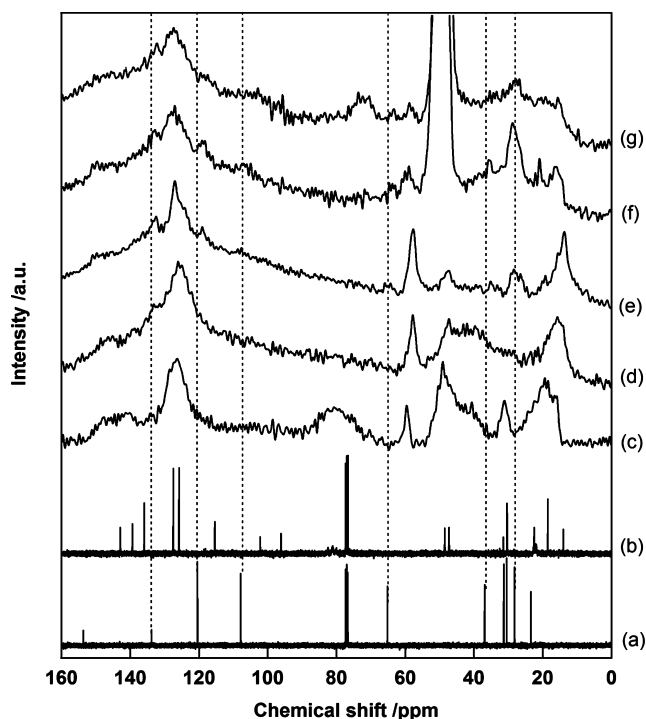


FIGURE 1. ^{13}C liquid and SS-NMR spectra of (a) **E** in CDCl_3 , (b) **B** in $\text{CDCl}_3/\text{CD}_3\text{OD}$ (4:1, v/v), (c) **C**, (d) **D**, (e) **F**, (f) **G_CVD**, and (g) **H_CVD**. Dashed lines indicate peaks attributed to **E**.

^{29}Si SS-NMR (Figure 2A) showed that the SiO_2 -matrix overlayers with the additives had considerably different compositions. When the SiO_2 -matrix overlayers were prepared without any additives, Q_2 ($\text{Si}(\text{OSi})_2(\text{OH})_2$; 11%, -91.7 ppm) and Q_3 ($\text{Si}(\text{OSi})_3(\text{OH})$; 56%, -100.8 ppm) Si species were observed, as well as Q_4 ($\text{Si}(\text{OSi})_4$; 34%, -109.2 ppm) Si species on **H_impreg** (Figure 2A(c)), indicating that the SiO_2 -matrix overlayers contain a substantial amount of unreacted Si–OH groups. The addition of a small amount of organic additive (e.g., IM-Si (1.0 wt % with respect to $\text{Si}(\text{OCH}_3)_4$)) significantly decreased the amount of Q_2 and Q_3 Si species (Figure 2A(e): 3% and 28%, respectively) and Q_4 Si species became the major species (69%) on **H_impreg IM-Si** (1.0 wt %), demonstrating that the basic additives acted as a catalyst for hydrolysis polymerization of TMOS. After the preparation of SiO_2 -matrix overlayers, a significant decrease in the intensity of Ru 3p X-ray photoelectron spectroscopy (XPS) peaks on **G** suggested that the space around the supported Ru complex was covered by the SiO_2 -matrix overlayers (Scheme 2).²⁸

Template (**E**) was successfully released from **G**; indeed 87% of template with respect to Ru was released from **G** with 1.0 wt % IM-Si, yielding a molecularly imprinted Ru complex (**H**) on the SiO_2 surface. In the ^{13}C SS-NMR spectrum, peaks attributable to **E** (28.2, 36.9, 65.2, 107.8, 120.4, and

133.8 ppm) disappeared from the SiO_2 -supported Ru complex. The step-by-step preparation of **H** with a reaction cavity suitable for the epoxidation of the terminal C=C bond of (*R*)-(+)-limonene was performed in a controlled manner, and the structures of the Ru complexes were characterized at each step.

We investigated the epoxidation of (*R*)-(+)-limonene on **H** with an imprinted reaction cavity matched to the template shape (Table 1). On **B**, the conversion of (*R*)-(+)-limonene was 93% and selectivities for the internal and terminal epoxide were 70% and 24%, respectively, after 24 h (entry 1). On **D**, similar conversion (90%) and selectivity (internal 62%; terminal 23%) were observed (entry 2). On the other hand, the epoxide selectivity was switched on **H**. The optimization of the temperatures of the hydrolysis polymerization and subsequent evacuation provided selectivities of 20% and 63% for the internal and terminal epoxides, respectively (91% conversion), and the terminal epoxide was obtained as a major product (Table 1 and Table S2, Supporting Information).

The shape-selective catalysis contributed to epoxidation of other alkene reactants (Table 2). The epoxidation of cyclopentene, cyclohexene, 1-hexene, and norbornene, which are smaller than limonene, smoothly proceeded on both **D** and **H_CVD** with similar conversions and selectivities, indicating that these reactants can easily enter the reaction cavity and the epoxidation reaction on **H_CVD** proceeds in a similar manner to **D**. In contrast, the reactions of alkene reactants, which are larger than the limonene and have different shapes from limonene, for instance, 1-heptene, cyclooctene, *trans*-2-octene, 5-vinyl-2-norbornene, and *trans*-stilbene, were suppressed on **H_CVD**, while the reaction proceeded on **D**, indicating that the imprinted catalyst prevented access of these reactants to the imprinted cavity, where the Ru center is located. These results demonstrate that molecularly imprinted Ru catalyst **H_CVD** has a reaction cavity for shape selectivity together with regioselectivity.

It is to be noted that the utilization of basic additives significantly improved the selectivity for the terminal epoxide on **H** (Table 1). The selectivity for the terminal epoxide was 73% on **H** prepared by the impregnation method without any additives (**H_impreg**), while that on **H** prepared by a similar impregnation method with 1.0 wt % $\text{NH}_2\text{-Si}$ (**H_impreg NH₂-Si** (1.0 wt %)) was 80% (entries 4 and 6). The best performance was obtained on **H_impreg IM-Si** (1.0 wt %); 91% conversion, 90% terminal epoxide selectivity (entry 11). The selectivity of (*R*)-(+)-limonene epoxidation on the imprinted catalyst was opposite that on the

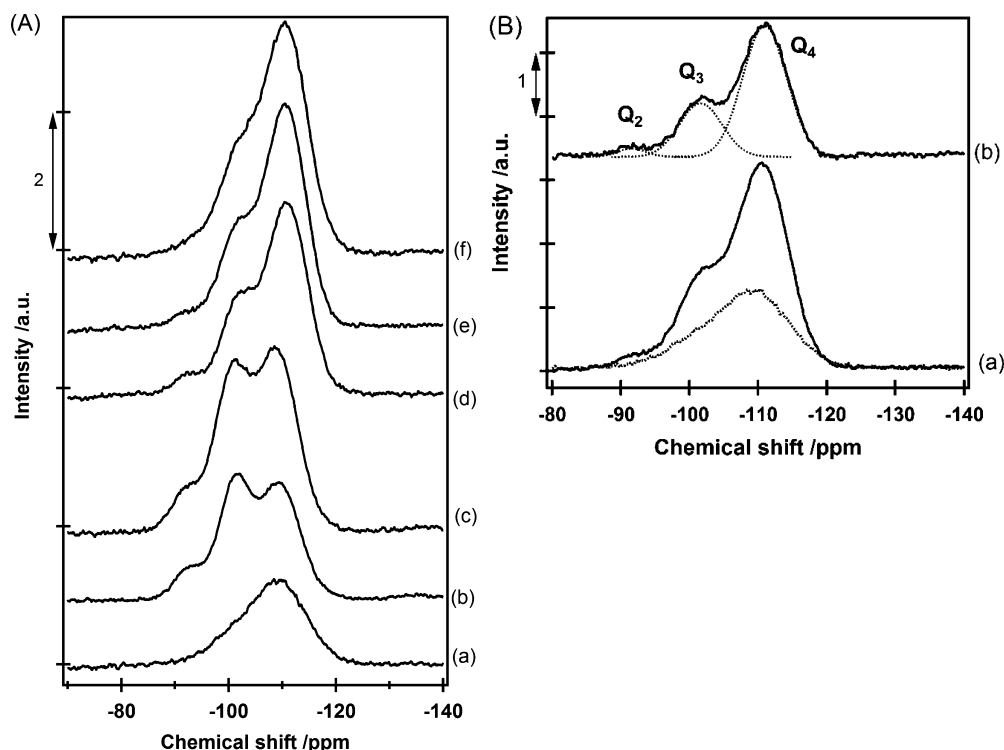


FIGURE 2. (A) ^{29}Si SS-NMR of (a) **D**, (b) **H_CVD**, (c) **H_Impreg**, (d) **H_Impreg_IM-Si** (0.5 wt %), (e) **H_Impreg_IM-Si** (1.0 wt %), and (f) **H_Impreg_IM-Si** (2.0 wt %). (B) (a) Raw spectra of **D** (dotted line) and **H_Impreg_IM-Si** (1.0 wt %) (solid line) and their difference spectrum (**H_Impreg_IM-Si** (1.0 wt %) – **D**) (solid line) and (b) fitted curves attributed to Q_2 , Q_3 , and Q_4 Si species (dotted lines).

TABLE 1. Catalytic Performance of (*R*)-(+)-Limonene Epoxidation on **B**, **D**, and **H**^a



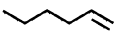

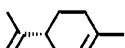

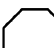
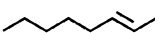
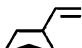
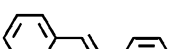
entry	catalyst	additive for polymerization of TMOS ^b	conv % (24 h)	selec %		
				internal	terminal	di
1	B (Homogeneous)		93	70	24	6
2	D (Supported)		90	62	23	15
3 ^{c,d}	H_CVD		91	20	63	17
4 ^c	H_impreg		96	19	73	8
5 ^c	H_impreg_NH₃	1.0 wt % NH ₃	98	25	64	11
6 ^c	H_impreg_NH₂-Si	1.0 wt % NH ₂ -Si	89	19	80	1
7 ^c	H_impreg_NMe₃	1.0 wt % NMe ₃	98	20	70	10
8 ^c	H_impreg_NMe₂-Si	1.0 wt % NMe ₂ -Si	96	18	81	1
9 ^c	H_impreg_2-MeIM	1.0 wt % 2-MeIM	81	29	61	10
10 ^c	H_impreg_IM-Si	0.5 wt % IM-Si	90	15	83	2
11 ^c		1.0 wt % IM-Si	91	9	90	1
12 ^c		1.5 wt % IM-Si	92	15	81	4
13 ^c		2.0 wt % IM-Si	54	23	73	4
14 ^c	H_impreg_p-styryl-Si	1.0 wt % <i>p</i> -styryl-Si	95	21	77	2
15 ^c	H_impreg_IL-Si	1.0 wt % IL-Si	99	27	67	6
16 ^c	H_impreg_DMAP-Si	1.0 wt % DMAP-Si	92	27	72	1
17 ^c	H_impreg_MAP	1.0 wt % MAP	22	37	63	0
18 ^{c,e}	H_impreg_IM-Si	1.0 wt % IM-Si	14 (2 d) 39 (5 d) 76 (12 d) ^f	10 15 15	86 81 77	4 4 8

^aRu concentration 1.5×10^{-6} mol; Ru/(*R*)-(+)-limonene/IBA = 1/200/200 (molar ratio), 3 mL of CH₂Cl₂, 298 K, 101.3 kPa O₂. ^bAn additive was used for the impregnation of TMOS. ^cPrepared by the hydrolysis polymerization of TMOS at 338 K and subsequent evacuation at 368 K. ^dTMOS was deposited by CVD instead of impregnation. ^eRu concentration 1.5×10^{-6} mol; Ru/(*R*)-(+)-limonene/IBA = 1/400000/400000 (molar ratio), 3 L of CH₂Cl₂, 298 K, 101.3 kPa O₂. ^fTON (12 days) = 304 888.

homogeneous catalyst. Large turnover number (TON) of 3.0×10^4 with selectivity of 77% after 12 days was also achieved on **H** (entry 18).

The activation energies and reaction rates were found to be 64 ± 7 kJ mol⁻¹ and 7.6×10^{-4} s⁻¹ (internal) and 81 ± 5 kJ mol⁻¹ and 4.2×10^{-4} s⁻¹ (terminal), respectively, on **D**.

TABLE 2. Catalytic Performance of Alkene Epoxidation on **D** and **H_CVD**^a

Reactant	D			H_CVD ^b		
	Time / h	Conv. %	Epoxide selec. %	Time / h	Conv. %	Epoxide selec. %
	12	98	82	12	97	84
	7	90	62	7	92	67
	6	94	66	6	90	67
	7	>99	70	7	88	72
	24	95	62 (internal) 23 (terminal)	24	91	20 (internal) 63 (terminal)
	12	95	61	12	61	61
	9	94	80	9	30	83
	7	>99	77	7	12	80
	8	20	52	48	0	-
	8	100	90	12	0	-

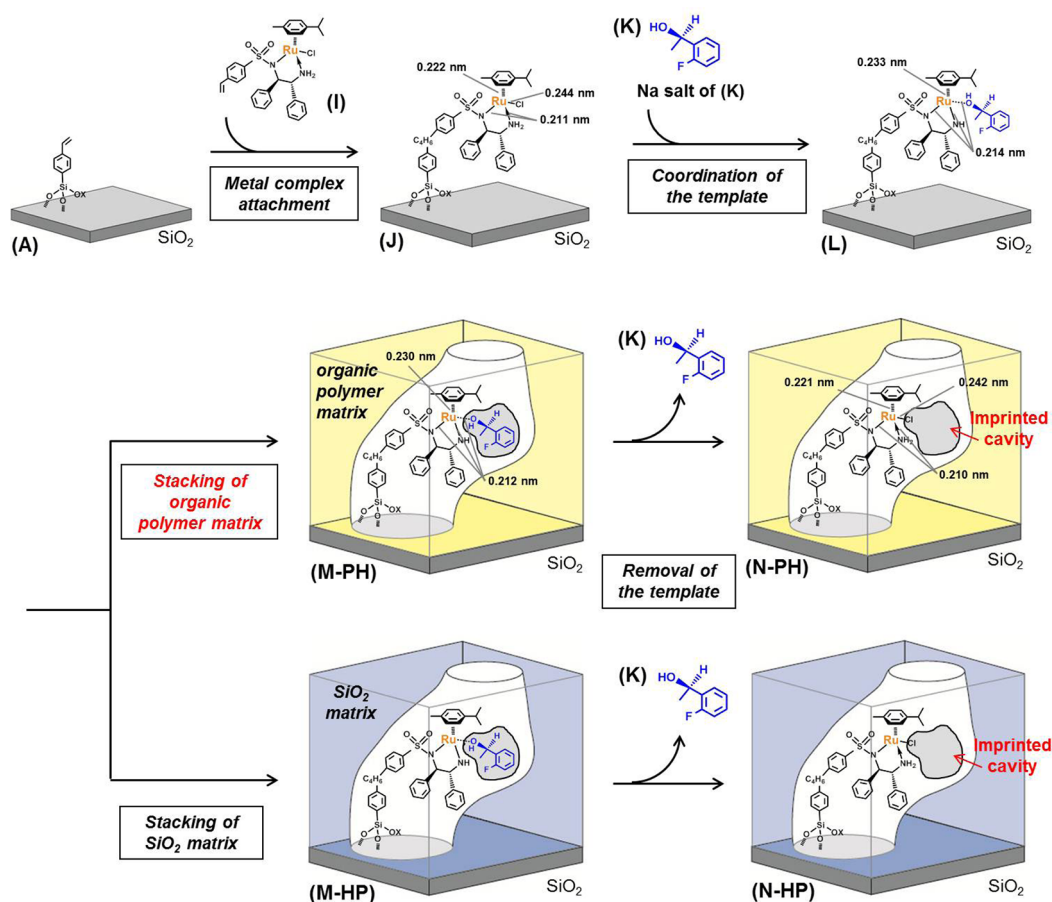
^aRu concentration 1.5×10^{-6} mol; Ru/reactant/IBA = 1/200/200 (molar ratio), 3 mL of CH_2Cl_2 , 298 K, 101.3 kPa O_2 . ^b**H_CVD** was prepared by the CVD method (hydrolysis polymerization at 338 K and subsequent evacuation at 368 K).

Compared with the terminal epoxide, the internal epoxide was formed 1.8-fold faster and had lower activation energy. These values on **H_impreg_IM-Si** (1.0 wt %) were 65 ± 7 kJ mol⁻¹ and 3.6×10^{-4} s⁻¹ (internal) and 35 ± 7 kJ mol⁻¹ and 15.8×10^{-4} s⁻¹ (terminal), respectively. Compared with the internal epoxide, the terminal epoxide formed 4.5-fold faster on **H_impreg_IM-Si** (1.0 wt %).

The reaction rate of internal epoxide formation was lower on **H_impreg_IM-Si** (1.0 wt %) than on **D**, but the activation energy of epoxidation of the internal alkene was almost the same on both **D** and **H_impreg_IM-Si** (1.0 wt %). These findings indicate that the epoxidation of the internal alkene was hindered due to the diffusion effect. In contrast, the activation energy of terminal alkene epoxidation on **H_impreg_IM-Si** (1.0 wt %) was about half that on **D**, and the rate of terminal epoxide formation was 3.8-fold higher on **H_impreg_IM-Si** (1.0 wt %) than on **D**. It is suggested that molecular imprinting not only suppresses the reaction rates of reactants shaped differently from the template but also has a possibility to raise the rates of template-shaped reactants.

3. Molecularly Imprinted Ru Catalysts in Organic Polymer Matrices for Transfer Hydrogenation in Aqueous Media

We have proposed molecular imprinting of an oxide-supported metal complex whose ligand is used as a template.^{26–29} We expanded this strategy to hydrogenation reactions in aqueous media by using hydrophobic organic polymer matrices instead of the SiO_2 -matrix overlayers.³⁰ Molecularly imprinted Ru complex catalysts for asymmetric transfer hydrogenation (ATH) of *o*-fluoroacetophenone in water were prepared by using hydrophobic polymer matrices as surface-matrix overlayers (Scheme 3).³⁰ The hydrophobic organic polymer matrices around the template created a hydrophobic reaction pocket, which was expected to serve as an efficient reaction site for shape-selective ATH reaction in water. One enantiomer produced by the hydrogenation of *o*-fluoroacetophenone, namely, (*R*)-1-(*o*-fluorophenyl)ethanol (**K**), was used as a template for ATH of *o*-fluoroacetophenone, and **K** was coordinated to SiO_2 -supported Ru complex (**J**).

SCHEME 3. Preparation of Molecularly Imprinted Ru Complex Catalysts on SiO₂ with Organic Polymer Matrices and SiO₂ Matrix for ATH of *o*-Fluoroacetophenone in Water

We used several methods to prepare matrix overlayers: (1) photopolymerization of ThreeBond 3026E containing acrylate oligomer and 2-hydroxyethyl methacrylate (method PH); (2) deposition polymerization of styrene and divinylbenzene (method VDP); (3) precipitation polymerization of methyl methacrylate and ethylene glycol dimethacrylate (method PP); and (4) hydrolysis polymerization of TMOS (method HP). The polymerization methods and height of deposited polymer matrices were evaluated by XPS, which is a practical way to investigate stacking manners of polymer matrices (Table 3). After the polymerization of an organic polymer on the surface of SiO₂, the intensity ratio of Si 2p XPS peak of SiO₂ to C 1s XPS peak of organic polymer decreases as the height of polymer matrix increases. If polymerization proceeds apart from the SiO₂ surface, the XPS peak intensity ratio is expected to be larger than that in the case of layer-by-layer polymerization when compared at a similar height of the polymer matrices, which was calculated from the observed densities of polymers prepared without SiO₂. The XPS peak intensity ratios were found to

be significantly different among the three polymerization methods (Table 3). When the height of polymer matrix was increased, the PH method brought about large decreases in the XPS peak intensity ratios. On the other hand, the degree of decrease in these values for **N_VDP** were smaller than those for **N_PH**, suggesting that monomers prepared by the VDP method would initially polymerize on SiO₂ but further polymerization tended to proceed apart from the SiO₂ surface. In the case of the PP method, the XPS peak intensity ratios were much larger than those of **N_PH** in every height. A significant decrease in the intensity of a Ru 3p XPS peak on **N_PH** (2 nm) supported the fact that space around the supported Ru complex was surrounded by the polymer-matrix overlayers.

Finally **K** was removed from **M** by the addition of triethylbenzylammonium chloride. The amount of **K** removed from **M_PH** (2 nm polymer height) was 0.89 equiv with respect to Ru, which was detected by GC. The local coordination of the molecularly imprinted Ru complex **N_PH** was investigated by Ru K-edge EXAFS to have

TABLE 3. XPS Peak Intensity Ratio (Si 2p/C 1s) and Catalytic Performance in Asymmetric Transfer Hydrogenation of *o*-Fluoroacetophenone of **I**, **J**, and **N**^{a,30}

catalyst	calculated polymer matrix height, nm ^b	XPS peak intensity ratio (Si 2p/C 1s)	conv %	% ee (<i>R</i>)
I			98	81
J			98	80
N_PH	0.5	1.48	>99	80
	1	1.27	99	90
	2	0.74	99	91
N_VDP	3	0.57	81	87
	0.5	1.59	42	80
	1	0.95	35	84
N_PP	2	0.86	21	87
	3	0.75	2	
	0.5	4.14	12	74
N_HP	1	2.28	8	62
	2	1.34	5	59
	3	0.99	3	54
	2		62	81

^aRu concentration 4×10^{-6} mol; Ru/SDS/*o*-fluoroacetophenone/HCOONa = 1/4/100/500; 2 mL water with SDS as a surfactant, 313 K, 96 h. The sum of them (mass balance) was 95–97%. ^bPolymer matrix heights were calculated using the observed density of each polymer.

coordination numbers (CNs) and bond distances similar to those of **J**, suggesting that template **K** on **N_PH** was released after the polymerization (Scheme 3). In contrast, the amount of released template was 0.77 and 0.64 per Ru on **M_VDP** and **M_PP**, respectively, implying that a part of the supported Ru complex was covered by the polymer matrices on **N_VDP** and **N_PP**.

Catalytic performance for ATH of *o*-fluoroacetophenone, whose hydrogenated product was imprinted, was investigated on the supported and molecularly imprinted catalysts in water (Table 3). On **I**, conversion and enantiomeric excess of *o*-fluoroacetophenone ATH was 98% and 81% ee (*R*), respectively, after 96 h. On **J**, similar conversion and enantiomeric excess were observed. On the molecularly imprinted catalysts, the catalytic activity was maintained on **N_PH** for polymer matrices of 0.5, 1, and 2 nm in height. Note that the enantiomeric excess of (*R*)-1-(*o*-fluorophenyl)-ethanol increased from 80% ee to 91% ee on **N_PH** with the polymer matrix of 2 nm in height. No further improvement of enantioselectivity was observed on **N_PH** with a polymer matrix of 3 mm in height.

In the cases of **N_VDP** and **N_PP**, the conversion and enantiomeric excess *o*-fluoroacetophenone were largely decreased, in accordance with the poor preparation of polymer matrix overlayers suggested by XPS analysis. It is to be noted that the conversion of *o*-fluoroacetophenone on **N_HP** with hydrophilic SiO₂-matrix overlayers prepared by hydrolysis polymerization of TMOS was much lower than on **J** or on **N_PH**. Hydrophilicity of the surface SiO₂-matrix overlayers

was suggested as a primary reason for the decrease in the catalytic activity on **N_HP**, and the hydrophobic PH polymer with partially hydrophilic OH groups may be involved in the modification of surface hydrophilicity, which would be advantageous for ATH in water.

4. Molecularly Imprinted Ru Catalyst with a Molecular Binding Site on the Imprinted Cavity Wall

Artificial design of an enzyme-like catalytic system requires not only creation of active metal species and a shape-selective reaction space but also design of spatially arranged molecular binding sites. Several attempts have been made to prepare molecular binding sites on imprinted materials using organic functional groups.^{17,18,35–39} We designed a molecularly imprinted Ru complex catalyst with a molecular binding site on the wall of a molecularly imprinted cavity.³¹

We prepared an NH₂ binding site on the wall of a molecularly imprinted cavity on a molecularly imprinted Ru complex on SiO₂. The target reaction was the shape-selective transfer hydrogenation of *o*-fluorobenzophenone (*o*-F-BP), which will have a favorable interaction with an NH₂ binding site at an appropriate spatial position. An alcohol similar in shape to the product of *o*-F-BP hydrogenation was coordinated to a SiO₂-supported Ru complex and was utilized as a template. A carbamate group (–NHCOO–) connected to a silane-coupling moiety (–Si(OC₂H₅)₃) was tethered to the alcohol template, and the cleavage of the carbamate moiety after affixing the silane-coupling moiety to the wall of the molecularly imprinted cavity produced a spatially arranged NH₂ binding site for the hydrogenation of *o*-F-BP (Scheme 4).

A template ligand (**O**) was initially coordinated to the Ru center of **J**. **O** is shaped like the product in the transfer hydrogenation and consists of three parts: an *o*-hydroxybenzhydrol moiety (**a**), which has a similar shape to the alcohol product of *o*-F-BP hydrogenation and is the object of the molecularly imprinted structure; a carbamate (–NHCOO–) linker (**b**); and a 3-triethoxysilylpropyl moiety (**c**), which is connected to imprinted object (**a**) via carbamate (**b**). New peaks attributed to **O** appeared in the ¹³C SS-NMR spectrum of **P-O** (Figure 3); for example, at 23 ppm for CH₂CH₂CH₂Si (**O-c**), 58 ppm for Si(OCH₂CH₃)₃ (**O-c**), 117 ppm for Ar (**O-a**), and 156 ppm for NHCOO (**O-b**).

Then, SiO₂-matrix overlayers of 1.8 nm in height were stacked by CVD, and subsequent hydrolysis polymerization of Si(OCH₃)₄ was performed.^{26–29} To explore the effects of

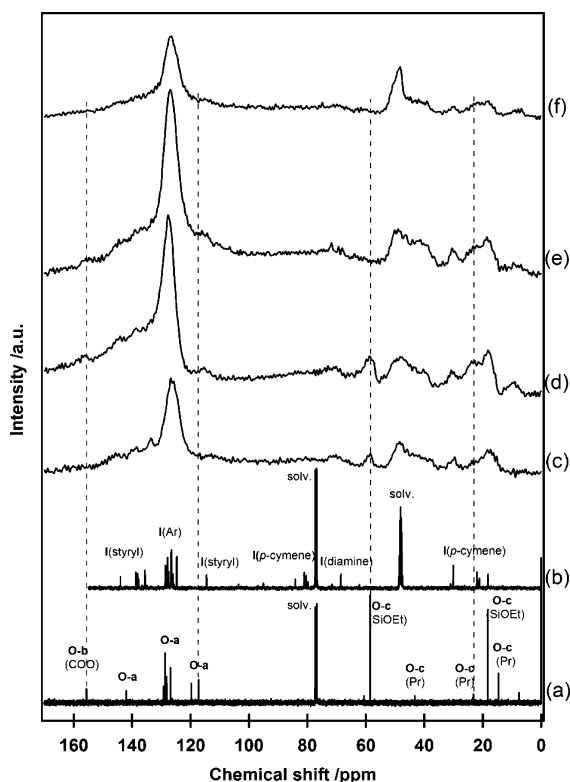


FIGURE 3. ^{13}C liquid- and SS-NMR spectra of (a) **O** in CDCl_3 , (b) **I** in $\text{CDCl}_3/\text{CD}_3\text{OD}$ (3:1, v/v), (c) **J**, (d) **P-O**, (e) **Q-O**, and (f) **R-BS**. Dashed lines indicate peaks attributed to **O**.

the template and NH_2 binding site, we prepared three samples with and without a template (Scheme 4). **R-noBS** was prepared by using *o*-methylbenzhydrol (**S**) as a template instead of **O**. The shape of **S** is similar to that of **O-a**, and thus an imprinted cavity with a similar shape to **O-a** without the NH_2 binding site could be prepared. **R-noTemp** was also prepared without any template on **J**. Similar amounts of SiO_2 -matrix overlayers were stacked in a similar way for the three catalysts **R-BS**, **R-noBS**, and **R-noTemp**. A large decrease in XPS peaks was observed (Figure 4), indicating that the SiO_2 -matrix overlayers stacked in the close proximity of the Ru complex.

The final step of the preparation of **R-BS** was the extraction of the template moiety (**O-a**) by the cleavage of the carbamate moiety (**O-b**) (to produce $-\text{NH}_2$, CO_2 , and $-\text{OH}$). In the ^{13}C SS-NMR spectrum of **Q-O**, the peak at 58 ppm for $\text{Si}(\text{OCH}_2\text{CH}_3)_3$ (**O-c**) disappeared in the preparation step from **P-O** to **Q-O** (Figure 3), indicating that the $\text{Si}(\text{OC}_2\text{H}_5)_3$ moiety of **O-c** was incorporated onto a part of the wall of the SiO_2 -matrix overlayers. Two peaks at 117 and 156 ppm for Ar (**O-a**) and NHCOO (**O-b**), respectively, disappeared in the preparation step from **Q-O** to **R-BS**, whereas the broad peak at around 23 ppm ($\text{CH}_2\text{CH}_2\text{CH}_2\text{Si}$ (**O-c**)) did not decrease in

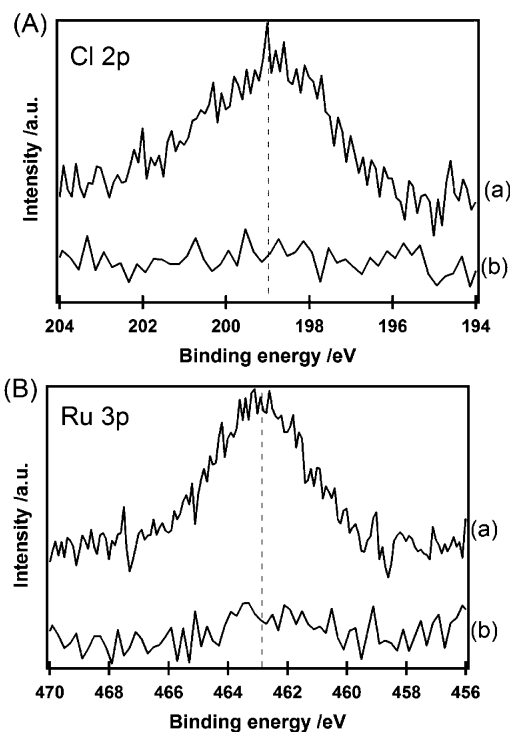
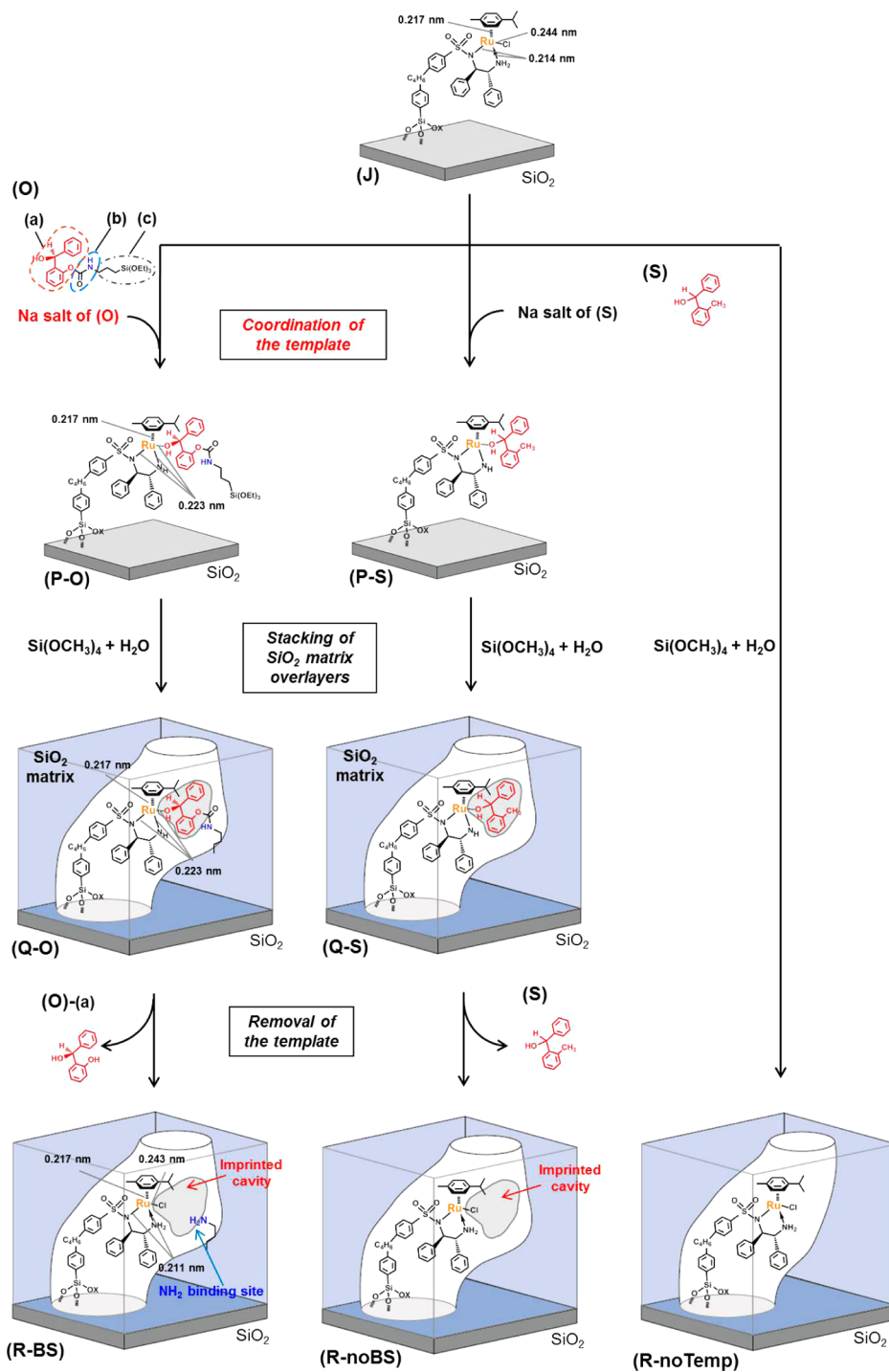


FIGURE 4. (A) Cl 2p XPS spectra of (a) **J** and (b) **P-O**. (B) Ru 3p XPS spectra of (a) **J** and (b) **R-BS**. Intensity was calibrated by the Si 2p peak intensity of each sample.

this step. These results indicate that **O-b** actually linked the *o*-hydroxybenzhydrol (**O-a**) and $\text{NH}_2(\text{CH}_2)_3$ moiety (**O-c**), that **O-a** was released from Ru in the final step by the cleavage of **O-b**, and that a cavity with a shape tailored to **O-a** in which an NH_2 binding site was fixed on the wall was created around the active Ru site (Scheme 4). The average diameter of the surface pores was estimated to be 0.82 nm by N_2 adsorption.

J exhibited enantioselectivity for ATH of *o*-F-BP (55% ee (*S*)) and *o*-methylbenzophenone (*o*-Me-BP) (71% ee (*S*)) (Table 4). After the removal of **O-a** by the cleavage of **O-b**, the transfer hydrogenation of *o*-F-BP proceeded with conversion of 29% in 4 days on **R-BS**-(1*R*,2*R*)-(*o*-*S*). **R-noTemp** did not exhibit any catalytic activity for the transfer hydrogenation. Thus, in the molecularly imprinted systems where the catalytic transfer hydrogenation did occur, the reaction proceeded within the template-shaped molecularly imprinted cavity. In the case of **R-noBS** with an imprinted cavity but without the NH_2 binding site, the activity of *o*-F-BP was lower than that on **R-BS** with the NH_2 binding site, but no significant differences were observed for *o*-Me-BP on **R-BS** and **R-noBS**.

The enantioselectivity of the transfer hydrogenation was a little higher in the molecularly imprinted system.

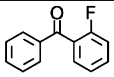
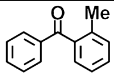
SCHEME 4. Steps for Preparing Molecularly Imprinted Ru Complex Catalysts on SiO₂ with and without an NH₂ Binding Site Spatially Arranged on the Wall of an Imprinted Cavity for ATH of *o*-Fluorobenzophenone

The enantiomeric excess for *o*-F-BP and *o*-Me-BP on **R-BS**-(1*R*,2*R*)-(1*S*) were 72% ee (*S*) and 79% ee (*S*), respectively, while those on **J** before imprinting were 55% ee (*S*) and 71% ee (*S*), respectively. The higher enantioselectivity might be caused by the overlayer wall restricting the mobility of the chiral diamine ligand on the Ru complex. The SiO₂-matrix

overlayers serve not only to create a molecular shaped cavity but also to regulate the flexibility of the coordinating ligands to enhance enantioselectivity.

The initial reaction rates for the transfer hydrogenation of *o*-F-BP, which can interact with the NH₂ binding site via hydrogen bonding, and *o*-Me-BP, which is not thought to

TABLE 4. Catalytic Performance of **I, J, P-O, Q-O, R-BS, R-noBS,** and **R-noTemp** in ATH of *o*-F-BP and *o*-Me-BP^{a,31}

Catalyst (catalyst)-(ligand)- (template) ^b	Time /d	Reactant			
					
		Conv. % (TOF /s ⁻¹)	%ee	Conv. %	%ee
I -(1 <i>R</i> ,2 <i>R</i>) (homogeneous)	1	98	54 (<i>S</i>)	35	68 (<i>S</i>)
J -(1 <i>R</i> ,2 <i>R</i>)	2	78 (4.4 × 10 ⁻⁴)	55 (<i>S</i>)	31	71 (<i>S</i>)
R-BS -(1 <i>R</i> ,2 <i>R</i>)-(o- <i>S</i>)	4	29 (8.3 × 10 ⁻⁵)	72 (<i>S</i>)	5	79 (<i>S</i>)
R-BS -(1 <i>S</i> ,2 <i>S</i>)-(o- <i>S</i>)	4	19	72 (<i>R</i>)	2	78 (<i>R</i>)
R-BS -(1 <i>R</i> ,2 <i>R</i>)-(p- <i>S</i>)	4	15	73 (<i>S</i>)	3	83 (<i>S</i>)
R-noBS -(1 <i>R</i> ,2 <i>R</i>)	4	14 (3.7 × 10 ⁻⁵)	71 (<i>S</i>)	6	78 (<i>S</i>)
R-noTemp -(1 <i>R</i> ,2 <i>R</i>)	4	0	-	0	-

^aRu⁴⁺/BuOK/reactant = 1/10/100 (molar ratio); [Ru] = 3.9 × 10⁻⁶ mol; *i*-PrOH 3 mL, 313 K. ^bLigand, (1*R*/*S*,2*R*/*S*)-*N*-*p*-styrenesulfonyl-1,2-diphenylethylenediamine; template, (*R*/*S*)-*o*/*p*-hydroxybenzhydrol.

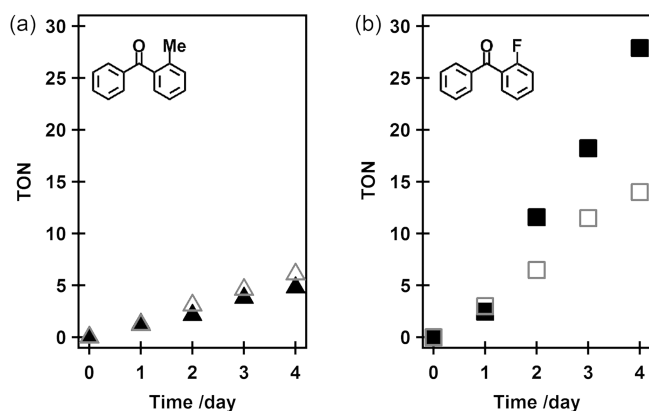


FIGURE 5. TONs of the transfer hydrogenation of (a) *o*-Me-BP and (b) *o*-F-BP on **R-BS**-(1*R*,2*R*)-(o-*S*) (▲, ■) with the NH₂ binding site and on **R-noBS**-(1*R*,2*R*) (△, □) without the NH₂ binding site at 313 K.

participate with the NH₂ binding site, were investigated. In the case of *o*-Me-BP, similar reaction rates were observed on **R-BS** and **R-noBS** (Figure 5a). On the other hand, the existence of the NH₂ binding site brought about an increase in the transfer hydrogenation activity for *o*-F-BP (Figure 5b). The reaction rate of *o*-F-BP on **R-BS** was twice that on **R-noBS**, implying that there was preferable adsorption of *o*-F-BP in the molecularly imprinted cavity in **R-BS** with the NH₂ binding site spatially arranged for the *o*-F-BP reactant. The coordination of the reactants to the Ru center may be a primary issue, but the interaction of the reactants with the NH₂ binding site via hydrogen bonding was also suggested to contribute on **R-BS**.

5. Summary and Outlook

In this Account, we focused on recent examples of molecularly imprinted Ru complex catalysts on SiO₂ surfaces, whose ligands were used as templates for the preparation of imprinted cavities on active Ru sites. The design of a template and surface matrix overlayers with a molecular binding site greatly affected the properties of the reaction cavity and, in turn, the catalytic selectivity. The molecular imprinting method utilizing supported metal complexes would be applicable for variety of catalytic reactions including syntheses of pharmaceuticals and functional molecules. The integration of various functional units for selective catalysis is an important issue to be addressed in the future, for instance, the molecular imprinting of a transition state structure of a reaction and the addition of several molecular binding sites inside a reaction cavity to achieve superior molecular recognition properties, to realize artificial enzymatic catalyst systems on surfaces toward 100% selective catalysis.

The authors thank Dr. Yong Yang, Dr. Zhihuan Weng, Mr. Mutsuo Kinoshita, and Mr. Nozomu Ishiguro at IMS for their collaboration. A part of this work was financially supported by the Funding Program for Next Generation World-Leading Researchers, JST Research Seeds Program, NEDO GSC Project, and Inoue Foundation for Science. XAFS measurements were performed with the approval of PF-PAC (No. 2005G209, 2008G154, 2010G020, and 2011G177).

Supporting Information. Experimental procedures for molecularly imprinted SiO₂-supported Ru complexes for regioselective epoxidation, Ru K-edge EXAFS data for the

prepared catalysts, the catalytic performances for regioselective epoxidation, and calculation methods for the height of surface matrix overlayers. This material is available free of charge via the Internet at <http://pubs.acs.org>.

BIOGRAPHICAL INFORMATION

Satoshi Muratsugu received his Ph.D. from Department of Chemistry, Graduate School of Science, at The University of Tokyo in 2009 under the supervision of Prof. Hiroshi Nishihara. After graduation, he joined the Institute for Molecular Science in 2009 as an assistant professor. He is currently working on design of new heterogeneous catalysts using supported transition metal complexes and clusters, design of molecularly imprinted metal complex catalysts, and preparation of alloy nanoparticle catalysts on oxide surfaces.

Mizuki Tada received her Ph.D. from The University of Tokyo in 2005 under the supervision of Professor Yasuhiro Iwasawa. She worked as an Assistant Professor at the Department of Chemistry, The University of Tokyo, from 2004 to 2008. In 2008, she became an Associate Professor at The University of Tokyo and moved to the Institute for Molecular Science. She has studied surface design of heterogeneous catalysts using metal complexes and in situ time-resolved/space-resolved XAFS characterization of heterogeneous catalysts under catalyst working conditions.

FOOTNOTES

The authors declare no competing financial interest.

REFERENCES

- Koniyama, M.; Takeuchi, T.; Mukawa, T.; Asanuma, H. *Molecular Imprinting*, Wiley-VCH Verlag GmbH & Co. KGaA: Weinheim, Germany, 2003.
- Yan, M.; Ramström, O., Eds. *Molecularly Imprinted Materials: Science and Technology*, Marcel Dekker: New York, 2005.
- Haupt, K.; Mosbach, K. Molecularly Imprinted Polymers and Their Use in Biomimetic Sensors. *Chem. Rev.* **2000**, *100*, 2495–2504.
- Holthoff, E. L.; Bright, F. V. Molecularly Imprinted Xerogels as Platforms for Sensing. *Acc. Chem. Res.* **2007**, *40*, 756–767.
- Maier, N. M.; Lindner, W. Chiral Recognition Applications of Molecularly Imprinted Polymers: A Critical Review. *Anal. Bioanal. Chem.* **2007**, *389*, 377–397.
- Ye, L.; Mosbach, K. Molecular Imprinting: Synthetic Materials as Substitutes for Biological Antibodies and Receptors. *Chem. Mater.* **2008**, *20*, 859–868.
- Cutivet, A.; Schembri, C.; Kovensky, J.; Haupt, K. Molecularly Imprinted Microgels as Enzyme Inhibitors. *J. Am. Chem. Soc.* **2009**, *131*, 14699–14702.
- Bui, B. T. S.; Haupt, K. Molecularly Imprinted Polymers: Synthetic Receptors in Bioanalysis. *Anal. Bioanal. Chem.* **2010**, *398*, 2481–2492.
- Hoshino, Y.; Koide, H.; Urakami, T.; Kanazawa, H.; Kodama, T.; Oku, N.; Shea, K. J. Recognition, Neutralization, and Clearance of Target Peptides in the Bloodstream of Living Mice by Molecularly Imprinted Polymer Nanoparticles: A Plastic Antibody. *J. Am. Chem. Soc.* **2010**, *132*, 6644–6645.
- Urraca, J. L.; Aureliano, C. S. A.; Schillinger, E.; Esselmann, H.; Wiltfang, J.; Sellergren, B. Polymeric Complements to the Alzheimer's Disease Biomarker β -Amyloid Isoforms A β 1–40 and A β 1–42 for Blood Serum Analysis under Denaturing Conditions. *J. Am. Chem. Soc.* **2011**, *133*, 9220–9223.
- Davis, M. E.; Katz, A.; Ahmad, W. R. Rational Catalyst Design via Imprinted Nanostructured Materials. *Chem. Mater.* **1996**, *8*, 1820–1839.
- Polborn, K.; Severin, K. Biomimetic Catalysis with Immobilised Organometallic Ruthenium Complexes: Substrate- and Regioselective Transfer Hydrogenation of Ketones. *Chem.—Eur. J.* **2000**, *6*, 4604–4611.
- Wulff, G. Enzyme-Like Catalysis by Molecularly Imprinted Polymers. *Chem. Rev.* **2002**, *102*, 1–27.
- Tada, M.; Iwasawa, Y. Design of Molecular-Imprinting Metal-Complex Catalysts. *J. Mol. Catal. A: Chem.* **2003**, *199*, 115–137.
- Becker, J. J.; Gagné, M. R. Exploiting the Synergy between Coordination Chemistry and Molecular Imprinting in the Quest for New Catalysts. *Acc. Chem. Res.* **2004**, *37*, 798–804.
- Burri, E.; Öhm, M.; Dagueuet, C.; Severin, K. Site-Isolated Porphyrin Catalysts in Imprinted Polymers. *Chem.—Eur. J.* **2005**, *11*, 5055–5061.
- Liu, J.; Wulff, G. Functional Mimicry of Carboxypeptidase A by a Combination of Transition State Stabilization and a Defined Orientation of Catalytic Moieties in Molecularly Imprinted Polymers. *J. Am. Chem. Soc.* **2008**, *130*, 8044–8054.
- Wulff, G.; Liu, J. Design of Biomimetic Catalysts by Molecular Imprinting in Synthetic Polymers: The Role of Transition State Stabilization. *Acc. Chem. Res.* **2012**, *45*, 239–247.
- Resmini, M. Molecularly Imprinted Polymers as Biomimetic Catalysts. *Anal. Bioanal. Chem.* **2012**, *402*, 3021–3026.
- McMorn, P.; Hutchings, G. J. Heterogeneous Enantioselective Catalysts: Strategies for the Immobilisation of Homogeneous Catalysts. *Chem. Soc. Rev.* **2004**, *33*, 108–122.
- Corma, A.; Garcia, H. Silica-Bound Homogeneous Catalysts as Recoverable and Reusable Catalysts in Organic Synthesis. *Adv. Synth. Catal.* **2006**, *348*, 1391–1412.
- Notestein, J. M.; Katz, A. Enhancing Heterogeneous Catalysis through Cooperative Hybrid Organic-Inorganic Interfaces. *Chem.—Eur. J.* **2006**, *12*, 3954–3965.
- Tada, M.; Iwasawa, Y. Advanced Chemical Design with Supported Metal Complexes for Selective Catalysis. *Chem. Commun.* **2006**, 2833–2844.
- Copéret, C.; Basset, J.-M. Strategies to Immobilize Well-Defined Olefin Metathesis Catalysts: Supported Homogeneous Catalysis vs. Surface Organometallic Chemistry. *Adv. Synth. Catal.* **2007**, *349*, 78–92.
- Thomas, J. M.; Raja, R. Exploiting Nanospace for Asymmetric Catalysis: Confinement of Immobilized, Single-Site Chiral Catalysts Enhances Enantioselectivity. *Acc. Chem. Res.* **2008**, *41*, 708–720.
- Tada, M.; Sasaki, T.; Iwasawa, Y. Performance and Kinetic Behavior of a New SiO₂-Attached Molecular-Imprinting Rh-Dimer Catalyst in Size- and Shape-Selective Hydrogenation of Alkenes. *J. Catal.* **2002**, *211*, 496–510.
- Tada, M.; Sasaki, T.; Iwasawa, Y. Novel SiO₂-Attached Molecular-Imprinting Rh-Monomer Catalysts for Shape-Selective Hydrogenation of Alkenes: Preparation, Characterization and Performance. *Phys. Chem. Chem. Phys.* **2002**, *4*, 4561–4574.
- Tada, M.; Sasaki, T.; Shido, T.; Iwasawa, Y. Design, Characterization and Performance of a Molecular Imprinting Rh-Dimer Hydrogenation Catalyst on a SiO₂ Surface. *Phys. Chem. Chem. Phys.* **2002**, *4*, 5899–5909.
- Tada, M.; Sasaki, T.; Iwasawa, Y. Design of a Novel Molecular-Imprinted Rh-Amine Complex on SiO₂ and its Shape-Selective Catalysis for α -Methylstyrene Hydrogenation. *J. Phys. Chem. B* **2004**, *108*, 2918–2930.
- Weng, Z.; Muratsugu, S.; Ishiguro, N.; Ohkoshi, S.; Tada, M. Preparation of Surface Molecularly Imprinted Ru-Complex Catalysts for Asymmetric Transfer Hydrogenation in Water Media. *Dalton Trans.* **2011**, *40*, 2338–2347.
- Yang, Y.; Weng, Z.; Muratsugu, S.; Ishiguro, N.; Ohkoshi, S.; Tada, M. Preparation and Catalytic Performances of a Molecularly Imprinted Ru-Complex Catalyst with an NH₂ Binding Site on a SiO₂ Surface. *Chem.—Eur. J.* **2012**, *18*, 1142–1153.
- Tada, M.; Coquet, R.; Yoshida, J.; Kinoshita, M.; Iwasawa, Y. Selective Formation of a Coordinatively Unsaturated Metal Complex at a Surface: A SiO₂-Immobilized, Three-Coordinate Ruthenium Catalyst for Alkene Epoxidation. *Angew. Chem., Int. Ed.* **2007**, *46*, 7220–7223.
- Tada, M.; Akatsuka, Y.; Yang, Y.; Sasaki, T.; Kinoshita, M.; Motokura, K.; Iwasawa, Y. Photoinduced Reversible Structural Transformation and Selective Oxidation Catalysis of Unsaturated Ruthenium Complexes Supported on SiO₂. *Angew. Chem., Int. Ed.* **2008**, *47*, 9252–9255.
- Tada, M.; Muratsugu, S.; Kinoshita, M.; Sasaki, T.; Iwasawa, Y. Alternative Selective Oxidation Pathways for Aldehyde Oxidation and Alkene Epoxidation on a SiO₂-Supported Ru-Monomer Complex Catalyst. *J. Am. Chem. Soc.* **2010**, *132*, 713–724.
- Katz, A.; Davis, M. E. Molecular Imprinting of Bulk, Microporous Silica. *Nature* **2000**, *403*, 286–289.
- Fireman-Shoresh, S.; Avnir, D.; Marx, S. General Method for Chiral Imprinting of Sol-Gel Thin Films Exhibiting Enantioselectivity. *Chem. Mater.* **2003**, *15*, 3607–3613.
- Liu, J.; Wulff, G. Functional Mimicry of the Active Site of Carboxypeptidase A by a Molecular Imprinting Strategy: Cooperativity of an Amidinium and a Copper Ion in a Transition-State Imprinted Cavity Giving Rise to High Catalytic Activity. *J. Am. Chem. Soc.* **2004**, *126*, 7452–7453.
- Zhang, H.; Piacham, T.; Drew, M.; Patek, M.; Mosbach, K.; Ye, L. Molecularly Imprinted Nanoreactors for Regioselective Huisgen 1,3-Dipolar Cycloaddition Reaction. *J. Am. Chem. Soc.* **2006**, *128*, 4178–4179.
- Bass, J. D.; Solovoyov, A.; Pascall, A. J.; Katz, A. Acid-Base Bifunctional and Dielectric Outer-Sphere Effects in Heterogeneous Catalysis: a Comparative Investigation of Model Primary Amine Catalysts. *J. Am. Chem. Soc.* **2006**, *128*, 3737–3747.